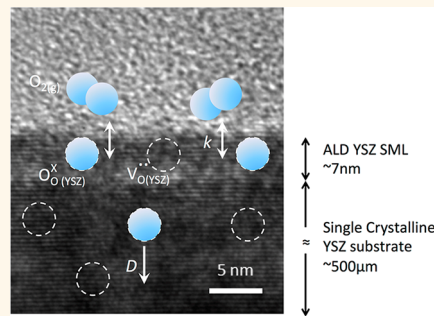


# Enhanced Oxygen Exchange on Surface-Engineered Yttria-Stabilized Zirconia

Cheng-Chieh Chao,<sup>†,‡,\*</sup> Joong Sun Park,<sup>†,‡,§,\*</sup> Xu Tian,<sup>§</sup> Joon Hyung Shim,<sup>‡</sup> Turgut M. Gür,<sup>||</sup> and Fritz B. Prinz<sup>†,||</sup>

<sup>†</sup>Department of Mechanical Engineering, Stanford University, Stanford, California 94305, United States, <sup>‡</sup>Environmental Energy Technologies Division, Lawrence Berkeley National Laboratory, Berkeley, California 94720, United States, <sup>§</sup>Department of Applied Physics, Stanford University, Stanford, California 94305, United States, <sup>||</sup>Department of Mechanical Engineering, Korea University, Seoul, Korea, and <sup>||</sup>Department of Materials Science and Engineering, Stanford University, Stanford, California 94305, United States. <sup>\*</sup>These authors equally contributed to the work.

**ABSTRACT** Ion conducting oxides are commonly used as electrolytes in electrochemical devices including solid oxide fuel cells and oxygen sensors. A typical issue with these oxide electrolytes is sluggish oxygen surface kinetics at the gas–electrolyte interface. An approach to overcome this sluggish kinetics is by engineering the oxide surface with a lower oxygen incorporation barrier. In this study, we engineered the surface doping concentration of a common oxide electrolyte, yttria-stabilized zirconia (YSZ), with the help of atomic layer deposition (ALD). On optimizing the dopant concentration at the surface of single-crystal YSZ, a 5-fold increase in the oxygen surface exchange coefficient of the electrolyte was observed using isotopic oxygen exchange experiments coupled with secondary ion mass spectrometer measurements. The results demonstrate that electrolyte surface engineering with ALD can have a meaningful impact on the performance of electrochemical devices.

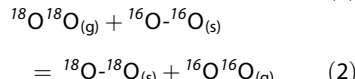
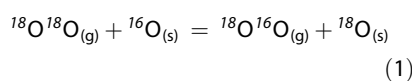


**KEYWORDS:** atomic layer deposition · oxygen isotope exchange/depth profiling · secondary ion mass spectrometry · solid oxide fuel cells

Ionically conducting oxides are essential components of various types of solid-state electrochemical devices. In solid oxide fuel cells (SOFCs) and oxygen sensors, these oxides selectively conduct oxide ions through oxygen vacancies and are commonly employed as electrolytes.<sup>1,2</sup> One of the key limitations for these oxides is the sluggish oxygen surface kinetics at the gas–electrolyte interface, which significantly hinders oxygen incorporation. Hence, optimizing the surface kinetics of these oxides is crucial for improving the electrochemical performance.

Early results of oxygen exchange studies using mass spectrometric analyses of the isotopic composition of the gas phase over various oxide surfaces have been compiled by Winter<sup>3</sup> and reviewed extensively by Boreskov and Novakova.<sup>4,5</sup> Ignoring homogeneous (*i.e.*, homophase) exchange within the gas phase, which is not relevant to the present study, two mechanistic pathways for the heterophase exchange reactions between the oxide surface and the gas phase oxygen isotope were postulated. One involves exchange between the molecular

oxygen isotope (*i.e.*,  $^{18}\text{O}^{18}\text{O}_{(\text{g})}$ ) and a single atom on the oxide surface (*i.e.*,  $^{16}\text{O}_{(\text{s})}$ ), while the other mechanism involves two atoms in the solid oxide ( $^{16}\text{O}–^{16}\text{O}_{(\text{s})}$ ) participating in the exchange reaction. The net reactions for single and multiple exchange can be summarized respectively by



These reactions are envisioned to occur at the outermost surface layers of oxides involving the cooperative participation of triatomic or tetra-atomic surface and subsurface oxygen intermediates.<sup>6</sup> As expected, oxygen exchange is a thermally activated process. Isotopic exchange depth profiling measurements on yttria-stabilized zirconia (YSZ) and gadolinia-doped ceria (GDC) using secondary ion mass spectrometry (SIMS) indicated an abrupt change in the activation energy for exchange at around 700 °C, from 0.7 eV (67 kJ/mol) for YSZ and 0.6 eV (58 kJ/mol) for GDC below 700 °C to 2.3 eV

\* Address correspondence to ccchao1@stanford.edu; joongspark@lbl.gov.

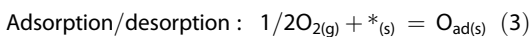
Received for review November 2, 2012 and accepted February 11, 2013.

Published online February 12, 2013  
10.1021/nn305122f

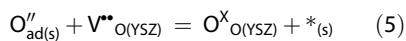
© 2013 American Chemical Society

(222 kJ/mol) for YSZ and 3.3 eV (318 kJ/mol) for GDC above 700 °C.<sup>7</sup> Interestingly, high-temperature values for the activation energies are nearly half the value for the corresponding band gaps for YSZ and GDC, suggesting that the availability of electrons during exchange at temperatures above 700 °C may be rate limiting. Exchange parameters such as activation energy and exchange rate may depend on various factors including the electrostatic lattice energy, impurity segregation, surface basicity, the heat of formation of the oxide, oxygen-to-oxygen lattice distance, and the pretreatment history of the oxide prior to exchange. For example, Winter<sup>8</sup> reported the activation energy for isotopic exchange on  $\text{ZrO}_2$  that was pretreated in a vacuum at 550–650 °C to be 63 kJ/mol, while this value doubles to 125 kJ/mol for pretreatment in oxygen, suggesting that the role of oxygen vacancies at or near the surface may be important. Winter also reported that the activation energy of 77 kJ/mol for isotopic oxygen exchange on  $\text{Y}_2\text{O}_3$  pretreated in oxygen is significantly lower than for  $\text{ZrO}_2$ , while the measured exchange rates for  $\text{Y}_2\text{O}_3$  pretreated in oxygen or in a vacuum were consistently higher than on  $\text{ZrO}_2$ . More recently, surface-sensitive low-energy ion scattering (LEIS) studies on YSZ clearly demonstrated the impact of impurities and impurity phases segregating to external surfaces and grain boundaries and forming a blocking layer that impedes oxygen exchange.<sup>9,10</sup> Furthermore, isotopic oxygen exchange measurements by SIMS on ion-implanted YSZ single-crystal surfaces have shown that Bi and Ce implantation enhanced the exchange coefficient at 700 °C.<sup>11</sup> These results collectively suggest that the nature of surface termination and the presence of ionic and electronic defects are important for the exchange properties of YSZ.

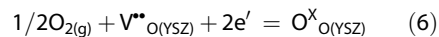
Reactions 1 and 2 represent a simplistic picture of the overall exchange process since both involve several intermediate steps including the dissociative adsorption of molecular  $^{18}\text{O}_2$  or  $^{18}\text{O}^{16}\text{O}$  on the oxide surface and, correspondingly, the associative desorption of either  $^{16}\text{O}^{16}\text{O}$  or  $^{18}\text{O}^{16}\text{O}$  from the oxide surface. There is no direct evidence that summary reactions 1 and 2 proceed via simple chemical exchange between the gas phase oxygen and the oxide ion residing on the outer surface of the solid oxide without the participation of electronic and ionic defects. Assuming single exchange for simplicity and ignoring the isotope notations, the overall exchange reaction most likely involves the following intermediate steps.



Incorporation :



Net reaction :



Here,  $*_{(\text{s})}$  indicates a surface site for adsorption,  $\text{O}_{\text{ad}(\text{s})}''$  denotes a doubly electronated oxygen on the oxide surface,  $\text{V}^{*}_{\text{O}(\text{YSZ})}$  represents an oxygen vacancy in YSZ, and  $\text{O}_{\text{O}(\text{YSZ})}^{\text{X}}$  is a lattice oxygen in YSZ in Kroger–Vink notation. So the oxygen exchange process is expected to involve the participation of vacancies, which constitutes the testing premise of the present study.

Dopant segregation to YSZ and GDC surfaces and grain boundaries has been reported previously.<sup>12–14</sup> Recent theoretical work<sup>15</sup> and surface-sensitive LEIS measurements<sup>16</sup> have provided strong evidence that dopant cations segregate to surfaces accompanied with the segregation of oxygen vacancies. Accordingly, we postulate that engineered YSZ surfaces enrich the availability of vacancies at the surface, leading to enhanced kinetics of oxygen exchange. The present study is designed to test this hypothesis.

YSZ is considered to be one of the most common electrolyte materials for SOFCs.<sup>17</sup> The slow oxygen exchange kinetics of YSZ at low temperatures is a critical bottleneck to reducing the operating temperature of SOFCs. One major material property of YSZ electrolyte is the yttria doping concentration, which is typically 8 mol % for maximizing oxygen ion conductivity.<sup>18,19</sup> This doping concentration affects the oxygen ion vacancy concentration in the electrolyte, which in turn affects oxygen exchange and transport properties. The oxygen surface exchange coefficient is a measure of the neutral oxygen exchange flux across the surface of the electrolyte, where the availability of oxygen vacancies plays a role in the exchange process (see reaction 5). Moreover, previous studies on mixed conducting oxides have shown a “near linear” relationship between the surface vacancy concentration and oxygen surface exchange coefficient.<sup>20,21</sup> By locally changing the doping concentration at the electrolyte surface, it is possible to tune the oxygen exchange property without affecting the oxygen transport property (oxygen ion conductivity) of the electrolyte. In a previous study, Chao *et al.* improved the electrochemical performance of an SOFC by introducing ALD YSZ surface modifications.<sup>22</sup> This preliminary finding indicated that ALD can be an effective tool to engineer the surface of YSZ electrolytes.

In this study, we explored the effects of surface engineering, by depositing YSZ surface modification layers (SMLs) on a single-crystal YSZ electrolyte. With the help of isotope exchange/depth profiling (IEDP) using SIMS, we acquired detailed information about surface exchange and transport properties of our surface-modified YSZ electrolytes. This information helped us identify the SML recipe that produced the highest surface exchange coefficient, which can be

used to improve the oxygen exchange kinetics at the electrode/electrolyte interface for SOFCs. In particular, the oxygen exchange kinetics at the interface was enhanced up to 300% by adding 5 to 10 nm of a surface modified layer.

## RESULTS AND DISCUSSION

To maintain a consistent platform for comparing the effect of SML recipes, we used impurity-free polished single-crystalline YSZ as test substrates (500  $\mu\text{m}$  thick, 8 mol % yttria doping, (100) surface orientation, surface roughness  $<5\text{ \AA}$ ) and followed a well-controlled procedure to prepare the surface-modified YSZ samples for the isotope tracer experiment. By analyzing the oxygen isotope tracer profile, we determined the surface oxygen exchange coefficient and the oxygen isotope self-diffusion coefficient of the surface-modified YSZ electrolyte. This approach is commonly used in solid-state electrolytes, for characterizing surface exchange and transport properties.<sup>7,11,20,23–31</sup>

Deposition of YSZ followed the recipes listed in Figure 1a. Each ALD YSZ SML had 10 repeats of a “supercycle”, and each supercycle contained eight ALD cycles of zirconia or yttria. The doping concentration in the SML was simply controlled by the number of yttria cycles contained in the supercycle. Figure 1b shows the correlation between the SML recipe and the measured yttria doping concentration after ALD cycles. The recipe 1Y7Zr produced a doping concentration similar to the YSZ substrates (6–8 mol %). The thickness of the 10-supercycle SML was approximately 7 nm, as shown in the cross section TEM (Figure 1c). A detailed characterization of ALD YSZ film morphology and crystallinity is reported elsewhere.<sup>32</sup>

The SMLs with different doping concentrations were relatively thin compared to the electrolyte (7 nm vs 500  $\mu\text{m}$ ), so that only the surface properties of the electrolyte were affected. The surface-modified electrolytes were subsequently infused for 2 h in a 150 Torr oxygen isotope atmosphere ( $^{18}\text{O}_2$ ) at 200, 250, and 300  $^{\circ}\text{C}$  and analyzed with SIMS depth profiling to acquire the oxygen isotope tracer profile.

To analyze the isotope tracer profiles, we constructed a one-dimensional model for oxide ion isotope diffusion. The diffusion profiles were calculated by solving the diffusion equation

$$\frac{\partial c_{18}}{\partial t} = \frac{\partial}{\partial x} \left( D_{18} \frac{\partial c_{18}}{\partial x} \right)$$

with the boundary conditions

$$k(c_g - c_{18}|_{x=0}) = -D_{18} \frac{\partial c_{18}}{\partial x} \Big|_{x=0} \quad \text{and} \quad c_{18}|_{x=L} = c_{bg}$$

where  $k$  denotes the surface exchange coefficient,  $c_g$  denotes the  $^{18}\text{O}$  isotope fraction in gas phase,  $c_{bg}$  denotes the natural abundance of the  $^{18}\text{O}$  isotope, and

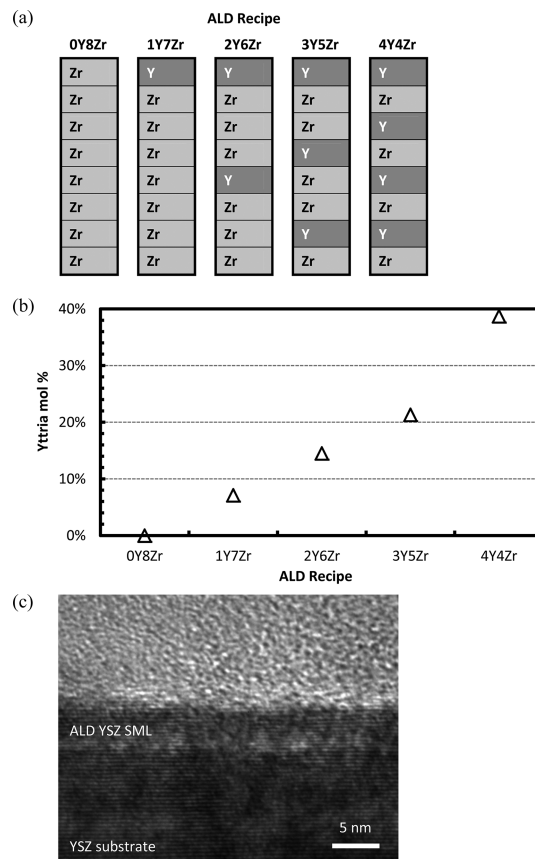


**Figure 1.** ALD YSZ SML recipes for modifying the YSZ electrolyte surface. (a) ALD recipes of YSZ surface-modified layer (SML). Each recipe contains one supercycle, and each supercycle contains eight ALD cycles of zirconia or yttria. (b) Yttria mol % in YSZ SML as a function of ALD recipe. (c) Cross section TEM of 10-supercycle SML deposited on a YSZ substrate. The thickness of the ALD YSZ SML is approximately 7 nm.

$L$  denotes the sample thickness. Diffusivity of the  $^{18}\text{O}$  isotope is defined by a step function:

$$D_{18} = \begin{cases} D_s & \text{at } 0 < x \leq s \\ D_{bulk} & \text{at } s < x \leq L \end{cases}$$

The solution was computed with COMSOL Multiphysics 3.5a, a commercial finite element analysis (FEA) software package. Diffusivity ( $D_{18}$ ) and surface exchange coefficient ( $k$ ) values were allowed to change to obtain a least-squares fit to the experimental data. For benchmarking, the isotope tracer profile of a “reference” YSZ sample (single-crystalline YSZ without the SMLs) is overlaid with the other fitting results in Figures 2 and 3.

We extracted  $D_{18}$  ( $D_{bulk}$ ) and  $k$  of the surface-modified electrolytes with different SML recipes (0Y8Zr, 1Y7Zr, 2Y6Zr, 3Y5Zr, 4Y4Zr), and the fitted diffusivity values are well matched with a previously reported value.<sup>26</sup> The introduction of SMLs did not affect the oxygen transport property of the YSZ electrolyte (Figure 2b). However, the surface exchange property demonstrated a strong correlation to the SML recipe (Figure 2c). The surface exchange coefficient,  $k$ , in

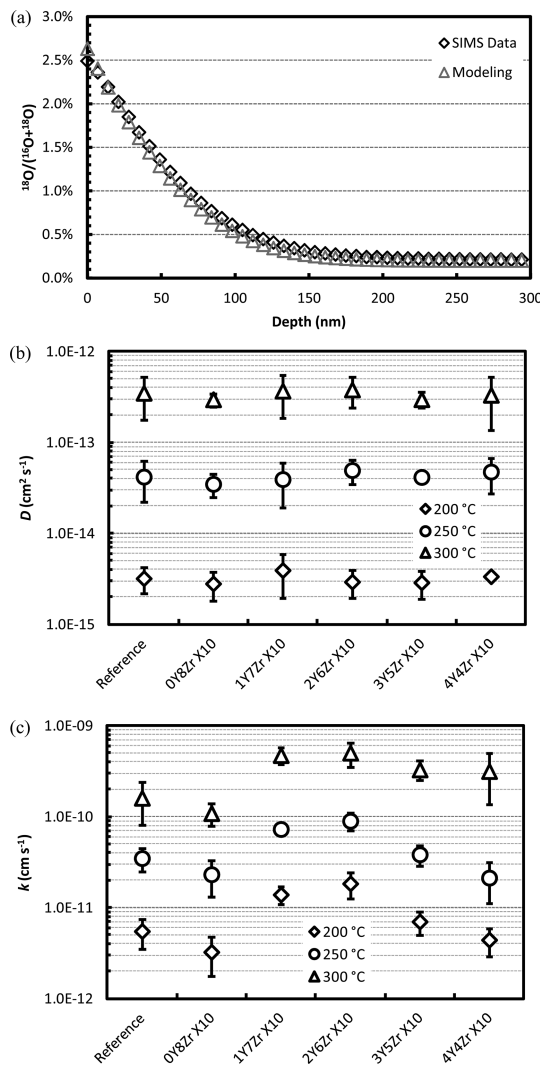


**Figure 2.** Oxygen exchange and transport properties as a function of SML recipes. Each SML contains 10 supercycles of repeating recipe. (a) Oxygen isotope tracer profile of reference YSZ electrolyte annealed at 200 °C overlapped with fitting result from analytical equation for extracting  $D_{18}$  and  $k$ . (b)  $D_{18}$  and (c)  $k$  of surface-modified YSZ electrolyte as a function of SML recipe annealed in isotope at 200, 250, and 300 °C.

the 0Y8Zr sample decreased compared with the reference because pure zirconia covered the surface. This is in agreement with earlier reports that indicated the activation energy for exchange on  $\text{ZrO}_2$  is larger than on  $\text{Y}_2\text{O}_3$ .<sup>8</sup> The  $k$  value increased as the yttria doping concentration increased and has the highest  $k$  values for the 2Y6Zr recipe, and this agrees well with previous studies.<sup>20,21</sup> The recipe 2Y6Zr produced up to three times higher  $k$  across three different isotope annealing temperatures compared to the reference sample. The  $k$  values decreased as we further increased the yttria doping concentration (3Y5Zr and 4Y4Zr). At these high yttrium doping levels, the mobile vacancy concentration is likely reduced due to defect interactions including association. This SML has a yttria doping concentration of 14 mol % (2Y6Zr), which is

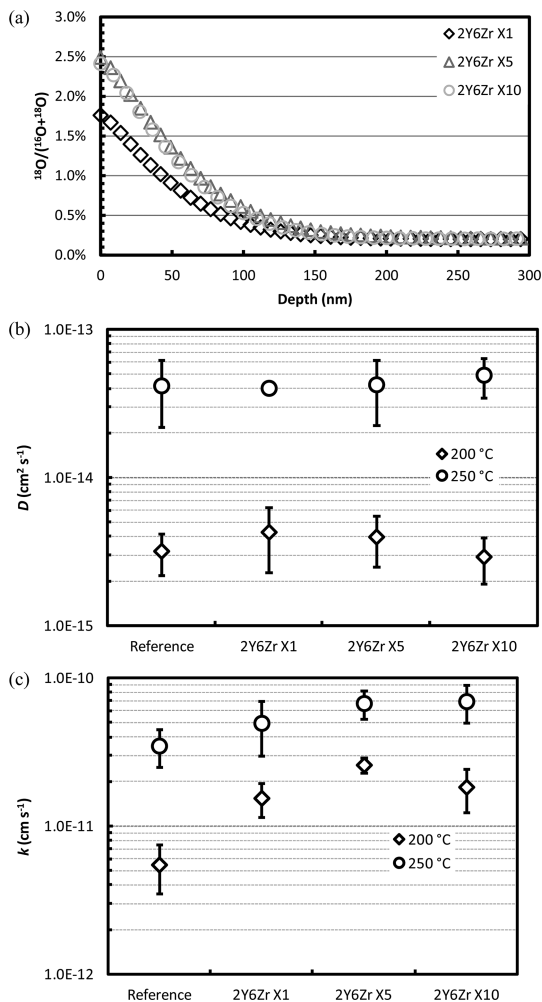


**Figure 3.** Oxygen exchange and transport properties as function of SML thickness. Recipe 2Y6Zr is used in all SMLs. (a) Oxygen isotope tracer profile as a function of the number of supercycles. Samples are annealed in oxygen isotope at 200 °C. (b)  $D_{18}$  and (c)  $k$  of surface-modified YSZ electrolyte as a function of the number of supercycles annealed in isotope at 200 and 250 °C.

significantly higher than the optimum doping level of 8 mol % known to yield the highest bulk conductivity value for oxide ions in YSZ. We speculate this divergence was contributed by the different requirements for surface exchange versus bulk transport with respect to the optimal yttria doping levels. The surface roughness contribution to  $k$  is small, since the surface roughness difference between samples is negligible. These results are well matched with electrochemical performances of YSZ samples with SMLs reported earlier.<sup>22</sup> One theory explaining why improved oxygen exchange kinetic is found in samples with highly doped surfaces points to impurity segregation or to the formation of a yttria-enriched layer at the YSZ subsurface as discussed earlier.<sup>9</sup> We ruled out the possibility of impurity segregation because not only does ALD involve pure precursors and provide a clean environment that eliminates the possibility of introducing impurities during deposition, but also cations do not have

enough mobility during ALD cycles or isotope annealing at these low processing temperatures below 300 °C. Hence, enhanced oxygen surface exchange kinetics are attributed to increased vacancy content in the SMLs.

In addition, we derived the activation energies of the surface-modified YSZ electrolytes. No significant difference in the activation energy was observed with different SML recipes. The activation energies of diffusivity and surface exchange were ~1.1 and ~0.8 eV, respectively, which were similar to the previously reported values for YSZ.<sup>7,8,33</sup>

Upon identifying the optimal surface doping concentration, we then characterized the effect of SML thickness by varying the total thickness of SML of a defined composition. Accordingly, we fixed the SML recipe as 2Y6Zr and deposited one, five, or 10 supercycles on the YSZ electrolytes. The sample preparation, isotope annealing, and SIMS analysis procedure were kept identical with the previous sample preparation procedure. The samples with five and 10 supercycles produced similar isotope tracer profiles, with 10 supercycles showing slightly lower isotope concentration. The sample with one supercycle produced the lowest isotope concentration (Figure 3a). We suspect that this was because the ALD YSZ SML coverage was not complete at one supercycle. As the number of supercycles increased to five, the surface was covered with ALD YSZ. With further increasing the number of supercycles to 10, the surface characteristics remained similar to five supercycles with full ALD YSZ coverage.

A similar conclusion can be drawn from the surface exchange property of the samples with different SML thicknesses (Figure 3c). The  $k$  of the YSZ electrolyte increased with one supercycle, increased further with five supercycles, and saturated with 10 supercycles. The  $k$  was up to five times higher than that for the reference sample. This result suggested that we do not need more than five supercycles to cover the surface of the YSZ electrolyte for improving the surface properties.

## CONCLUSION

In summary, with the help of IEDP, we studied the surface of the electrolyte with quantitative evidence of the surface doping effect, which helped us better understand the correlation between surface exchange kinetics and surface doping concentration. We verified that the addition of SML significantly enhances the oxygen exchange kinetics at the electrolyte surface without any negative impact on the oxygen transport. The SML that produced the optimal surface exchange coefficient was five supercycles of 2Y6Zr, which corresponds to less than 10 nanometers of 14 mol % yttria doped YSZ layer. This result indicated that the optimal doping concentration at the surface required for enhanced oxygen exchange is in fact different from that required for fast transport through the bulk of the YSZ electrolyte. Consequently, it is indeed beneficial to have a slightly higher doping concentration at the surface than in the bulk to optimize both oxygen exchange and transport properties of the electrolyte.

## METHODS

**Sample Preparation.** Single-crystal 8% yttria-stabilized zirconia substrates with (100) surface orientation were obtained from MTI Crystals. The YSZ substrates were chemical mechanical polished to a surface roughness of <5 Å and precut to a 25 × 25 × 0.5 mm sample size. For the isotope annealing, substrates were diced into 5 × 10 × 0.5 mm pieces, using a low-speed diamond saw. The substrates were first cleaned in a Piranha solution (sulfuric acid/hydrogen peroxide = 3:1) to remove surface contaminants, then immediately coated with ALD YSZ SML to ensure a good bonding of SML to the YSZ substrate.

The SML deposition followed the recipes listed in Figure 1a. Each recipe contained eight ALD cycles, with the yttria concentration tuned by the number of yttria cycles within each supercycle. The metal precursors used for the zirconia and yttria deposition were tetrakis(dimethylamino)zirconium(IV) (99.99%, Sigma-Aldrich) and tris(methylcyclopentadienyl)yttrium(III) (99.9%, Strem Chemicals), respectively. The oxidant used was distilled water. The deposition of the SML was done at 250 °C in a laboratory prototype ALD reactor.

**Oxygen Isotope Exchange.** The SML samples were placed into a quartz tube reactor, heated to 200, 250, and 300 °C, and preannealed in research grade oxygen (purity 5.0) at 150 Torr for more than 6 h. After preannealing, the dosing chamber was evacuated and immediately backfilled with oxygen isotope ( $^{18}\text{O}_2$ , purity >99%) to a pressure of 150 Torr. The isotope annealing time is 2 h. After isotope annealing, the quartz tube was rapidly removed from the oven and quenched to room temperature. Preheating samples prior to dosing combined

with rapid quenching at the end ensured an accurate dosing time.

**Secondary Ion Mass Spectrometry.** SIMS analysis for the samples was performed with two devices: Phi 6600 (Evans Analytical Group, Surface Analysis Laboratory) and CAMECA IMS 7f-GEO (Caltech, Center for Microanalysis). In CAMECA 7f-GEO SIMS, a 20 nA, 10 keV  $\text{Cs}^+$  primary beam with normal incidence electron gun charge compensation was used in the analysis, and  $^{16}\text{O}$  and  $^{18}\text{O}$  secondary ions were collected through the magnetic sector. The primary beam was rastered over a 100  $\mu\text{m} \times 100 \mu\text{m}$  area. In Phi 6600, a 5 keV  $\text{Cs}^+$  primary beam with 60° off-normal angle of incidence was used in the analysis, and  $^{16}\text{O}$  and  $^{18}\text{O}$  secondary ions were collected with a quadrupole mass analyzer. The depth of the etch crater was measured with a surface profiler (AlphaStep 500, KLA Tencor).

**Conflict of Interest:** The authors declare no competing financial interest.

**Acknowledgment.** We are grateful to Dr. Yunbin Guan and Prof. John Eiler of the Geology Department at California Institute of Technology (CalTech) for their assistance with and collaboration on the SIMS work. We would like to acknowledge Dr. Stephen P. Smith from Evans Analytical Group for his help with the Phi 6600 SIMS depth profiling, and Swagelok for providing high-temperature ALD valves. We thank Jihwan An for help with TEM experiments. J.S.P. acknowledges financial support from Samsung Scholarship. J.H.S. is grateful to the National Research Foundation (NRF) of the Korean Ministry of Education, Science and Technology (MEST) (Grant No. NRF-2010-0005810) for their financial support. T.M.G. and F.B.P. gratefully acknowledge

partial support from the Center on Nanostructuring for Efficient Energy Conversion (CNEEC) at Stanford University, an Energy Frontier Research Center funded by the U.S. Department of Energy, Office of Science, Office of Basic Energy Sciences, under Award Number DE-SC0001060.

*Note Added after ASAP Publication:* Due to a production error, this paper published ASAP on February 15, 2013 with a value missing in equation 3. The corrected version was reposted on February 25, 2013.

## REFERENCES AND NOTES

1. Steele, B. C. H. Oxygen Ion Conductors and Their Technological Applications. *Mater. Sci. Eng.* **1992**, *B13*, 79–87.
2. Dietz, H. Gas-Diffusion-Controlled Solid-Electrolyte Oxygen Sensors. *Solid State Ionics* **1982**, *6*, 175–183.
3. Winter, E. R. S. The Reactivity of Oxide Surfaces. *Adv. Catal.* **1958**, *10*, 196–241.
4. Boreskov, G. K. The Catalysis of Isotopic Exchange in Molecular Oxygen. *Adv. Catal.* **1965**, *15*, 285–339.
5. Novakova, J. Isotopic Exchange of Oxygen  $^{18}\text{O}$  between the Gaseous Phase and Oxide Catalysts. *Cat. Rev.-Sci. Eng.* **1971**, *4*, 77–113.
6. Martin, D.; Duprez, D. Mobility of Surface Species on Oxides: 1. Isotopic Exchange of  $^{18}\text{O}_2$  with  $^{16}\text{O}$  Of  $\text{SiO}_2$ ,  $\text{Al}_2\text{O}_3$ ,  $\text{ZrO}_2$ ,  $\text{MgO}$ ,  $\text{CeO}_2$ , and  $\text{CeO}_2\text{-Al}_2\text{O}_3$ . Activation by Noble Metals. Correlation with Oxide Basicity. *J. Phys. Chem.* **1996**, *100*, 9429–9438.
7. Manning, P. S.; Sirman, J. D.; Kilner, J. A. Oxygen Self-Diffusion and Surface Exchange Studies of Oxide Electrolytes Having Fluorite Structure. *Solid State Ionics* **1997**, *93*, 125–132.
8. Winter, E. R. S. Exchange Reactions of Oxides. Part IX. *J. Chem. Soc. A* **1968**, 2889–2902.
9. de Ridder, M.; VanWelzenis, R. G.; Brongersma, H. H.; Kreissig, U. Oxygen Exchange and Diffusion in the Near Surface of Pure and Modified Yttria-Stabilized Zirconia. *Solid State Ionics* **2003**, *158*, 67–77.
10. de Ridder, M.; Vervoort, A. G. J.; van Welzenis, R. G.; Brongersma, H. H. The Limiting Factor for Oxygen Exchange at the Surface of Fuel Cell Electrolytes. *Solid State Ionics* **2003**, *156*, 255–262.
11. Tannhauser, D. S.; Kilner, J. A.; Steele, B. C. H. The Determination of the Oxygen Self-Diffusion and Gas-Solid Exchange Coefficients for Stabilized Zirconia by SIMS. *Nucl. Instrum. Methods Phys. Res.* **1983**, *218*, 504–508.
12. Huang, H.; Gür, T. M.; Saito, Y.; Prinz, F. B. High Ionic Conductivity in Ultrathin Nanocrystalline Gadolinia-Doped Ceria Films. *Appl. Phys. Lett.* **2006**, *89*, 143107.
13. Lei, Y.; Ito, Y.; Browning, N. D. Segregation Effects at Grain Boundaries in Fluorite-Structured Ceramics. *J. Am. Ceram. Soc.* **2002**, *85*, 2359–2363.
14. Wang, X.-G. Yttrium Segregation and Surface Phases of Yttria-Stabilized Zirconia (111) Surface. *Surf. Sci.* **2008**, *602*, L5–L9.
15. Lee, H. B.; Prinz, F. B.; Cai, W. Atomistic Simulations of Surface Segregation of Defects in Solid Oxide Electrolytes. *Acta Mater.* **2010**, *58*, 2197–2206.
16. de Ridder, M.; van Welzenis, R. G.; van der Gon, A. W.; Brongersma, H. H.; Wulff, S.; Chu, W.-F.; Weppner, W. Subsurface Segregation of Yttria in Yttria Stabilized Zirconia. *J. Appl. Phys.* **2002**, *92*, 3056–3064.
17. Ivers-Tiffée, E.; Webera, A.; Herbstritta, D. Materials and Technologies for SOFC-Components. *J. Eur. Ceram. Soc.* **2001**, *21*, 1805–1811.
18. Kuwabara, M.; Murakami, T.; Ashizuka, M.; Kubota, Y.; Tsukidate, T. Electrical Conductivity of Yttria Partially Stabilized Zirconia Ceramics. *J. Mater. Sci. Lett.* **1985**, *4*, 467–471.
19. Pornprasertsuk, R.; Ramanarayanan, P.; Musgrave, C. B.; Prinz, F. B. Predicting Ionic Conductivity of Solid Oxide Fuel Cell Electrolyte from First Principles. *J. Appl. Phys.* **2005**, *98*, 103513–103518.
20. Kilner, J. A.; De Souza, R. A.; Fullarton, I. C. Surface Exchange of Oxygen in Mixed Conducting Perovskite Oxides. *Solid State Ionics* **1996**, *86–88*, 703–709.
21. Yasuda, I.; Hikita, T. Precise Determination of The Chemical Diffusion Coefficient of Calcium-Doped Lanthanum Chromites by Means of Electrical Conductivity Relaxation. *J. Electrochem. Soc.* **2009**, *141*, 1268–1273.
22. Chao, C.-C.; Kim, Y. B.; Prinz, F. B. Surface Modification of Yttria-Stabilized Zirconia Electrolyte by Atomic Layer Deposition. *Nano Lett.* **2009**, *9*, 3626–3628.
23. Kilner, J. A.; Steele, B. C. H.; Ilkov, L. Oxygen Self-Diffusion Studies Using Negative-Ion Secondary Ion Mass Spectrometry (SIMS). *Solid State Ionics* **1984**, *12*, 89–97.
24. Steele, B. C. H.; Kilner, J. A.; Dennis, P. F.; McHale, A. E.; van Hemert, M.; Burggraaf, A. J. Oxygen Surface Exchange and Diffusion in Fast Ionic Conductors. *Solid State Ionics* **1986**, *18*, 1038–1044.
25. Knorer, G.; Reimann, K.; Rower, R.; Sodervall, U.; Schaefer, H. Enhanced Oxygen Diffusivity in Interfaces of Nanocrystalline  $\text{ZrO}_2\text{-Y}_2\text{O}_3$ . *Proc. Natl. Acad. Sci. U.S.A.* **2003**, *100*, 3870–3873.
26. Huang, H.; Shim, J. H.; Chao, C.-C.; Pornprasertsuk, R.; Sugawara, M.; Gür, T. M.; Prinz, F. B. Characteristics of Oxygen Reduction on Nanocrystalline YSZ. *J. Electrochem. Soc.* **2009**, *156*, B392–B396.
27. De Souza, R. A.; Pietrowski, M. J.; Anselmi-Tamburini, U.; Kim, S.; Munir, Z. A.; Martin, M. Oxygen Diffusion in Nanocrystalline Yttria-Stabilized Zirconia: The Effect Of Grain Boundaries. *Phys. Chem. Chem. Phys.* **2008**, *10*, 2067–2072.
28. De Souza, R. A.; Kilner, J. A. Oxygen Transport in  $\text{La}_{1-x}\text{Sr}_x\text{Mn}_{1-y}\text{Co}_y\text{O}_{3-\delta}$  Perovskites: Part II. Oxygen Surface Exchange. *Solid State Ionics* **1999**, *126*, 153–161.
29. Lane, J. A.; Benson, S. J.; Waller, D.; Kilner, J. A. Oxygen Transport in  $\text{La}_{0.6}\text{Sr}_{0.4}\text{Co}_{0.2}\text{Fe}_{0.8}\text{O}_{3-\delta}$ . *Solid State Ionics* **1999**, *121*, 201–208.
30. Raj, E. S.; Kilner, J. A.; Irvine, J. T. S. Oxygen Diffusion and Surface Exchange Studies on  $(\text{La}_{0.75}\text{Sr}_{0.25})_{0.95}\text{Cr}_{0.5}\text{Mn}_{0.5}\text{O}_{3-\delta}$ . *Solid State Ionics* **2006**, *177*, 1747–1752.
31. Vannier, R. N.; Skinner, S. J.; Chater, R. J.; Kilner, J. A.; Mairesse, G. Oxygen Transfer in BIMEVOX Materials. *Solid State Ionics* **2003**, *160*, 85–92.
32. Shim, J. H.; Chao, C.-C.; Huang, H.; Prinz, F. B. Atomic Layer Deposition of Yttria-Stabilized Zirconia for Solid Oxide Fuel Cells. *Chem. Mater.* **2007**, *19*, 3850–3854.
33. Manning, P. S.; Sirman, J. D.; De Souza, R. A.; Kilner, J. A. The Kinetics of Oxygen Transport in 9.5 mol % Single Crystal Yttria Stabilized Zirconia. *Solid State Ionics* **1997**, *100*, 1–10.